Nonlocal transport hydrodynamic model for laser heated plasmas

Cite as: Phys. Plasmas **25**, 032704 (2018); https://doi.org/10.1063/1.5011818
Submitted: 03 November 2017 • Accepted: 20 February 2018 • Published Online: 07 March 2018

M. Holec, J. Nikl and S. Weber

Nonlocal transport hydrodynamic model for laser heated plasmas

M. Holec,[1,a)] J. Nikl,[2,3] and S. Weber[3]
[1]*Centre Lasers Intenses et Applications, Universite de Bordeaux-CNRS-CEA, UMR 5107, F-33405 Talence, France*
[2]*Faculty of Nuclear Sciences and Physical Engineering, Czech Technical University in Prague, Brehova 7, 115 19 Praha 1, Czech Republic*
[3]*ELI-Beamlines Institute of Physics, AS CR, v.v.i, Na Slovance 2, Praha 8 180 00, Czech Republic*

(Received 3 November 2017; accepted 20 February 2018; published online 7 March 2018)

The interaction of lasers with plasmas, whether pre-formed or due to ablation processes, very often takes place under nonlocal transport conditions. The nonlocality affects the transport of particles, mostly electrons, as much as it does radiation. In this study, the nonlocal transport is investigated for the plasma corona generated due to the deposition of laser energy. The nonlocal theory of the energy transport in radiative plasmas of the arbitrary ratio of the characteristic spatial scale length to the photon and electron mean free paths is applied to define closure relations of the hydrodynamic system. The corresponding transport phenomena cannot be described accurately with the usual fluid approach dealing only with local values and derivatives. Thus, the usual diffusive energy flux is instead calculated directly by solving a simplified transport equation allowing one to take into account the effect of long-range particle transport. The key feature of the proposed hydrodynamic closure is a direct solution of the simplified Bhatnagar-Gross-Krook form of the Boltzmann transport equation for electrons and the proper form of the radiation transport equation. *Published by AIP Publishing.* https://doi.org/10.1063/1.5011818

I. INTRODUCTION

The aim of this article is to use, and numerically solve, an appropriate nonlocal heat and radiation transport closure to the hydrodynamics equations in the context of laser-plasma interactions. Such a closure should be able to handle a wide range of Knudsen numbers $\mathrm{Kn} = \lambda/L$, where λ is the mean free path of either massive particles or photons and L the plasma inhomogeneity scale length. The number Kn is a fundamental quantity characterizing the type of transport regime.[1–6] A commonly used characteristic scale length is derived from the profile of the plasma electron temperature T_e (using its gradient ∇T_e) and can be defined as $L = \frac{T_e}{|\nabla T_e|}$ or as $L = \frac{1}{k}$, where k is the dominant component of the temperature profile in Fourier k-space. In principle, the characteristic scale length based on the profile of electron density n_e should also be included to address the transport regime, but since the standard hydrodynamic codes lean on the local heat flux approximation $\mathbf{q} \approx \nabla T_e$, we use the Knudsen number based on the electron temperature gradient of electrons $\mathrm{Kn}^e = \frac{\lambda^e |\nabla T_e|}{T_e} = k\lambda^e$, where λ^e is the electron mean free path. Consequently, the photon mean free path is defined as $\mathrm{Kn}^p = \frac{\lambda^p |\nabla T_e|}{T_e} = k\lambda^p$, where λ^p is the photon mean free path.

Typical transport regimes in laser heated plasmas can be divided into three domains being distinguished by the Knudsen number as follows:

- $\mathrm{Kn} > 10$: This regime of transport can be considered as free streaming. It is very common for photons in the under-critical ablative plasma, i.e., in the corona. It is very rare that the electrons enter this regime.
- $0.001 < \mathrm{Kn} < 10$: This regime of transport is called the nonlocal transport. It is typical for electrons in the corona. In the case of photons, it is rather present in the layer between critical density and ablation front (the so-called conduction zone).
- $\mathrm{Kn} < 0.001$: This regime is represented by a relatively cold and highly compressed material. It is opaque/collisional for most of the photons/electrons and this is where the Chapman-Enskog expansion method[7] applies and transport is always diffusive.

It is worth mentioning that the inhomogeneity length scale defined above is just an approximation. For example, a flat profile of temperature in the corona plasma can lead to an almost infinite length scale characteristic, and consequently, the Knudsen number would imply a diffusive regime. On the contrary, the scale length is limited by the extension of the corona and the transport of both electrons and photons is well described as ballistic. Also, the above description holds for "usual" particles; nevertheless, some extremes as fast electrons or X-ray photons can exhibit surprisingly high Knudsen numbers, which is naturally accompanied by the effect of high anisotropy of the transport.

In order to address the complex physics of nonlocality of transport, a new approach of nonlocal transport closure in hydrodynamics is presented, which leans on the idea of combining *physics* represented by the radiation transport and the linear Boltzmann transport equations and *numerics* providing their efficient and general multi-dimensional solution. Such a formulation enables the usage of arbitrary order discretization in both the space and the angle, achieving high-order accuracy and also the freedom in future extendibility of the physical model.

a)milan.holec@u-bordeaux.fr

In this paper, we provide an extensive overview of previously published nonlocal transport models in Sec. II. We further present details of a new nonlocal transport hydrodynamic model (NTH) aimed for laser-heated plasma simulations described in Sec. III. Section IV shows actual radiation-hydrodynamic simulations and reflects the nonlocal transport effect on hydrodynamic profiles of laser heated plasmas, where additional simulations providing the performance of a newly proposed nonlocal electron transport model against Fokker-Planck (FP) simulations are presented. A short conclusion is presented in Sec. V. Appendixes A and B present additional details concerning the physical relevance of the nonlocal electron transport model and its coupling to hydrodynamics, respectively.

II. PREVIOUS ATTEMPTS FOR MODELING NONLOCAL TRANSPORT IN HYDRODYNAMICS

As has been already mentioned, the most widely used model of heat transport in hydrodynamic codes is a local diffusion approximation given by heat conduction (also referred to as Fourier's law), which expresses the local thermal flux density $\mathbf{q} = -\kappa \nabla T_e$ to be equal to the product of thermal conductivity, κ, and the negative local temperature gradient $-\nabla T_e$. The pioneering work in the field of plasma physics was presented by Spitzer-Harm (SH),[8,9] which defines the thermal conductivity κ_{SH} for a high temperature plasma. This conductivity is based on the original Lorentz gas approximation (highly ionized Maxwellian plasma) extended by the heat conduction effect due to the electron-electron collisions.

Nevertheless, the simulation experience led to the necessary application of a heat flux limiter[10] due to the excessive overestimation of the heat flux in regions characterized by steep temperature gradients and low density (due to the long electron mean free path) typical for plasmas heated by lasers. A practical application of such a flux limiter resides in using a fraction of the local free-streaming limit $q_{fs} = n_e m_e v_{th}^3$, where m_e is the mass of the electron and $v_{th} = \sqrt{k_B T_e / m_e}$ the electron thermal velocity. In principle, this fraction can be varied between 0.02 (Ref. 11) and 0.15 (Ref. 12) with respect to the level of transport nonlocality best expressed by the Knudsen number and following the tendency that the stronger the nonlocality the smaller the fraction needs to be applied in order to provide reasonable plasma profiles. A general discussion about the detailed effect of the flux limiter variation was described in Ref. 13.

With the advent of the Fokker-Planck (FP) simulations of high-power laser generated plasmas,[14–18] the nonlocal nature of the heat flux was addressed. The question of the effect of transport nonlocality and anisotropy was studied in the FP simulations, and it was concluded that the first order Legendre expansion should be sufficient under the condition of steep temperature gradients.[15] It should be mentioned that the motion of ions and laser energy deposition were not included in the simulated problem. Since it was clear that the effect of nonlocality needs to be included in hydro codes, an answer how to treat the nonlocality of heat flux was provided by Luciani, Mora, and Virmont (LMV),[19] where they proposed that spatial convolution over the SH flux can address the necessary properties as flux inhibition and preheat observed in the FP simulations. Even though the LMV based simulations solved the previous problems of flux limitation, the necessity of an ad-hoc convolution kernel parameter based on the fit to FP simulations made it difficult to use the LMV model in hydrodynamic simulations. This shortage of the LMV model was improved by Albritton, Williams, Bernstein, and Swartz (AWBS).[20] Their approach resided in an analytical solution of a simplified form of the FP equation while considering suprathermal electrons. Consequently, they proposed an improved convolution kernel providing a better response to the FP simulations. Further improvement of the convolution approach including the treatment of the nonlocal electric field can be found in Ref. 21. The authors of Refs. 22 and 23 pointed out some serious issues inherently possessed by the numerical methods treating LMV and AWBS convolution models, which lead to nonphysical behavior. An overview of the accuracy and theoretical insight into LMV and AWBS convolution models can be found in Refs. 24 and 25. It was revealed that the nonphysical behavior was due to the thermal conductivity scaling $\kappa_{LMV/AWBS} = \kappa_{SH}/(k\lambda^e)^2$ when $k\lambda^e \to \infty$, where κ_{LMV} and κ_{AWBS} are the conductivities used in LMV and AWBS models. The work presented in Refs. 24 and 25 further extends the convolution model by proposing a new kernel based on k-space analysis of the effect of nonlocality, which possesses new properties, e.g., a correct dependence of nonlocal transport in the case of large Knudsen numbers, i.e., $\kappa_{FP} = \kappa_{SH}/(k\lambda^e)$ when $k\lambda^e \to \infty$, where κ_{FP} is the thermal conductivity.

In continuation with the k-space analysis, new analytical formulas for collisional and collisionless plasmas were proposed in Refs. 26–29. A different approach to solve the convolution delocalization based on[26] kernel was done in Refs. 30 and 31. This approach resides in solving the problem of energy equation (including the divergence of heat flux) in the Fourier space, thus providing a straightforward way of addressing nonlocal nature of the heat flux. In this case, the gradient of temperature is represented by k^α, where $\alpha = 1$. The concept of nonlocality leads to a decrease in the exponent, i.e., $0 < \alpha < 1$. The corresponding description can also be found in real space expressed by the fractional derivative model of the diffusion equation. In plasma physics, such an approach can be found in Ref. 32.

Even though the convolution strategy seemed to provide an acceptable solution to the nonlocal transport, its main drawback resides in its extension to more dimensions. Schurtz, Nicolai, and Busquet (SNB)[33] presented a new point of view to the problem of convolution. It is based on the similarity of the LMV convolution and the analytical solution of the linear transport equation, where the latter can be solved in multi-dimensions. Originally, the SNB model uses the model of the simplified Boltzmann transport equation proposed by Bhatnagar, Gross, and Krook (BGK)[5] and thus can be referred to as SNB-BGK. Further improvement of the SNB method including self-consistent electric and magnetic fields[34,35] or reformulating it to SNB-AWBS can be found in the literature.[36]

So far, the models evolving originally from heat conduction (Fourier's law) have been discussed. A common property of these is that they are based on extensions of the SH approach, which possess, by definition, the Chapman-Enskog small parameter expansion method.[7]

New methods based on the moments of a simplified Boltzmann transport equation (like BGK or AWBS) have been proposed quite recently.[36–38] These models are based on the first two angular moments, i.e., zero and first angular moment, where the system of equations is further completed by defining the necessary closure mimicking the next (second) angular moment of the simplified Boltzmann equation. The P1 closure[36] is based on the P1 approximation (first order Legendre expansion) of the electron distribution function, which leads to a very simple form of the closure being a linear function of the zero order moment. However, it was shown that such a closure exhibits a strong constraint on possible anisotropy of the transport.[36] A significant amount of work was done in order to improve the restriction on the transport anisotropy (inherent to P1 closure), by presenting the M1 closure,[36–39] which depends not only on the zero moment but also on the first moment, thus allowing any level of transport anisotropy. This nonlinear closure was originally developed for radiation transport by Minerbo.[40] The idea of the M1 closure resides in finding angular distribution, which maximizes angular entropy, i.e., a direct consequence of the second law of thermodynamics (equivalent to the Maxwell-Boltzmann distribution maximizing entropy of plasma).

A kinetic based model of nonlocal electron transport for hydrodynamic time-scales was introduced in Ref. 41. It is an analytical formulation solving the stationary Krook-type BGK Boltzmann transport equation, which derives from first principles Landau-Fokker-Planck electron-ion collisions (using a low anisotropy assumption, revised in Appendix A). However, the simplified form of the velocity dependent BGK collision operator violates fundamental conservation properties which are intimately related to transport, e.g., conservation of particles, momentum, and energy. A deeper theoretical insight into the acceptability of the velocity dependent BGK operator was further developed by Colombant–Manheimer–Goncharov (CMG) in Ref. 42, where the most important finding is that issue with the velocity dependence seems to be minimized if the hydrodynamics evolves on a much larger time scale than the kinetic time scale of electrons.

Even though our model is also based on the original BGK, the hydrodynamic scheme does conserve energy. This can be easily seen in the energy conservation equations of hydrodynamics (3) and (4) which strictly conserve the energy of the system, because the effect of nonlocal transport is given by the divergence of radiation and electron fluxes of energy, and consequently, no energy can be gained or drained by the system. The hydrodynamic numerical scheme we use[43] is strictly conservative in total mass and momentum without nonlocal corrections, which is not fundamentally inconsistent with the mechanism of the electron transport due to the high ion-electron mass ratio.

In the history of modeling the radiation transport, we can find some equivalents to the electron transport, e.g., the Rosseland radiative heat conduction,[44] which corresponds to the SH flux. However, its range of validity is extremely limited under the conditions of laser heated plasmas due to high Kn^p (in comparison to Kn^e) and the only remedy is to solve the fundamental radiation transfer equation.[1]

In principle, one can find in the literature two different approaches to model the transfer equation. The first approach is based on its moments, where, in general, just the first two moment equations regarding energy and momentum are considered, where additionally a set of higher moments could be applied, but the first two are widely used and considered to be sufficient.[45,46] An essential part of this approach is a closure of moments, where the well known *variable Eddington factor* (VEF) is well established in radiation transport modeling and naturally leads to the *radiation diffusion* model. VEF was originally developed in Ref. 47 and further improved in Refs. 40 and 48 in order to improve the anisotropy constraints and limit the nonphysically overestimated flux.

The second approach based on a direct solution of the radiation transfer equation referred to as discrete-ordinates or S_N usually relies on short-characteristic methods used to solve the problem of transport of particles. The pioneering work done by Carlson[49] and further applied by Pomraning[50] brought this method to public at an early stage. The problems associated with inaccuracy and negative solutions vanished through the use of the discontinuous finite element method.[51,52] The originally proposed strategy of obtaining the solution to the radiation transport equation resided in sweeping the intensity I along a set of discrete directions (ordinates). A further progress in acceleration of such sweeping methods was presented in Refs. 53 and 54. The modern form of the discontinuous finite element method is referred to as the discontinuous Galerkin (DG) method,[55–57] which offers a high-order discretization and computational efficiency capabilities.[58–60]

Based on the knowledge from the previously mentioned methods for electrons and radiation transport modeling, we propose a novel approach, which in an efficient way numerically solves the BGK Boltzmann transport equation for both photons and electrons, while these are inherently coupled to the bulk plasma fluid. Even though the additional dimensions of the phase space lead to a higher computational cost, a direct solution of the kinetic approach is worth doing it since it provides detailed information about the angular distribution (addressing any level of anisotropy) and does not lean on any approximation as Legendre or small parameter expansion. Furthermore, the simplicity of the linear BGK equation proposes a numerical stability of our developed high-order finite element scheme.[61]

III. NONLOCAL TRANSPORT HYDRODYNAMIC MODEL FOR LASER HEATED PLASMAS

A. Hydrodynamics

The *nonlocal transport hydrodynamic model* of laser-heated plasma refers to the two temperature single-fluid plasma model including laser-plasma coupling, nonlocal radiation-plasma coupling, and nonlocal electron-plasma coupling. Mass, momentum density, and total energy ρ, $\rho\mathbf{v}$, and $E = \frac{1}{2}\rho\mathbf{v}\cdot\mathbf{v} + \rho\varepsilon_i + \rho\varepsilon_e$, where ρ is the density of

plasma, $\mathbf{v}$ is the plasma fluid velocity, ε_i is the specific internal ion energy density, and ε_e is the specific internal electron energy density, are modeled by the Euler equations in the Lagrangian frame

$$\frac{\mathrm{d}\rho}{\mathrm{d}t} = -\rho\nabla\cdot\mathbf{v}, \tag{1}$$

$$\rho\frac{\mathrm{d}\mathbf{v}}{\mathrm{d}t} = -\nabla(p_i + p_e), \tag{2}$$

$$\rho\left(\frac{\partial\varepsilon_i}{\partial T_i}\frac{\mathrm{d}T_i}{\mathrm{d}t} + \frac{\partial\varepsilon_i}{\partial\rho}\frac{\mathrm{d}\rho}{\mathrm{d}t}\right) = -p_i\nabla\cdot\mathbf{v} - \nabla\cdot\mathbf{q}_i - G(T_i - T_e), \tag{3}$$

$$\rho\left(\frac{\partial\varepsilon_e}{\partial T_e}\frac{\mathrm{d}T_e}{\mathrm{d}t} + \frac{\partial\varepsilon_e}{\partial\rho}\frac{\mathrm{d}\rho}{\mathrm{d}t}\right) = -p_e\nabla\cdot\mathbf{v} - \nabla\cdot(\mathbf{q}_e + \mathbf{q}_R) + G(T_i - T_e) - \nabla\cdot\mathbf{q}_L, \tag{4}$$

where T_i is the temperature of ions, T_e is the temperature of electrons, p_i is the ion pressure, p_e is the electron pressure, $\mathbf{q}_i$ is the ion heat flux, $\mathbf{q}_e$ is the flux of energy due to electrons, $\mathbf{q}_R$ is the flux of energy due to radiation, $\mathbf{q}_L$ is the laser energy flux (Pointing vector), and $G = \rho\frac{\partial\varepsilon_e}{\partial T_e}\nu_e$ is the ion-electron energy exchange rate, where ν_e is the electron collision frequency. The thermodynamic closure terms p_e, p_i, $\frac{\partial\varepsilon_e}{\partial T_e}$, $\frac{\partial\varepsilon_i}{\partial T_i}$, $\frac{\partial\varepsilon_e}{\partial\rho}$, and $\frac{\partial\varepsilon_i}{\partial\rho}$ are obtained from the SESAME equation of state tables.[62,63]

The laser absorption model determines laser energy deposition, which appears as the explicit source term $\nabla\cdot\mathbf{q}_L$ on the right hand side of Eq. (4). In principle, any model of the laser plasma interaction used in hydrodynamic simulations can be incorporated into our NTH model. In this work, an efficient, yet physically relevant, 1D method solving the propagation of the laser in an inhomogeneous plasma, an algorithm based on stationary Maxwell's equations, which provides the Pointing vector $\mathbf{q}_L$ of the laser field, is employed.[64] It is based on the solution of the Helmholtz equation for the electric field $\mathbf{E}_L$ in 1D

$$\frac{\partial^2 E_L}{\partial z^2} = -\frac{\omega^2}{c^2}\varepsilon E_L,$$

where ω is the laser frequency, c the speed of light, E_L the transverse component of the electric field, and the relative complex permittivity ε reads[65]

$$\varepsilon = 1 - \frac{\omega_{pe}^2}{\omega(\omega + i\nu_e)},$$

where ω_{pe} stands for the electron plasma frequency. The electron collision frequency ν_e determines the efficiency of inverse-bremsstrahlung laser absorption. We use the global model of the electron collision frequency ν_e defined in Ref. 66, which provides a very useful interpolation over a wide range of temperatures during the pre-plasma formation. It is defined as

$$\nu_e = \min\left[\left(\nu_{ei}^{-1} + \nu_{el-phonon}^{-1}\right)^{-1}, \nu_{cut}\right],$$

where ν_{ei} is the electron-ion collision frequency described by the classical Spitzer-Harm formula,[9,67] $\nu_{el-phonon}$ is the solid state limit of electrons scattered by phonons,[68] and ν_{cut} is a frequency limitation providing that electrons cannot scatter on a spatial scale smaller than the ion sphere radius.[69]

So far, we have defined all the parts of the hydrodynamic model (1–4) except for the transport related term $\nabla\cdot(\mathbf{q}_e + \mathbf{q}_R)$. These are formulated via nonlocal transport closure of electrons and nonlocal transport closure of radiation in Secs. III C and III B.

B. Nonlocal radiation transport closure

The *nonlocal radiation transport hydrodynamic extension* is represented by the standard radiation transport equation[2]

$$\mathbf{n}\cdot\nabla I^p = \frac{aT_e^4 - I^p}{\lambda^p}, \tag{5}$$

where $I^p = \int f^p\,\frac{h^4\nu^3}{c^2}\,\mathrm{d}\nu$ is the one-group radiation intensity (the energy integrated photon distribution function f^p, where ν is the photon frequency and h is the Planck constant) and λ^p is the photon mean free path based on the mean Planck opacity presented in Ref. 70. The time derivative term of the radiation transport equation (5) can be neglected in the laser-heated plasmas.[2] The *nonlocal radiation transport closure* providing the energy flux reads

$$\mathbf{q}_R = \int_{4\pi}\mathbf{n}I^p\,\mathrm{d}\mathbf{n},$$

where I^p is the one group radiation intensity computed from Eq. (5).

C. Nonlocal electron transport closure

Based on the theory of radiation hydrodynamics[1] and, in particular, the pioneering work of Bhatnagar *et al.*,[5] the electron transport in plasmas can be described as

$$\frac{\partial f^e}{\partial t} + \mathbf{u}\cdot\nabla f^e + \frac{q_e}{m_e}\mathbf{n}\cdot\mathbf{E}\frac{\partial f^e}{\partial|\mathbf{u}|} = \frac{n_i}{n_e}\frac{\mathrm{d}\bar{Z}}{\mathrm{d}t}f_M + \nu_e(f_M - f^e), \tag{6}$$

where f^e is the distribution function of electrons, $\mathbf{u} = \mathbf{n}|\mathbf{u}|$ is the electron velocity in given direction $\mathbf{n}$ with magnitude $|\mathbf{u}|$, $\mathbf{E}$ is a plasma generated electric field, $\frac{\mathrm{d}\bar{Z}}{\mathrm{d}t}$ is the source of free electrons due to the ionization change rate (provided by the individual electron model of the BADGER equation of state library[71]), and f_M is the Maxwell-Boltzmann distribution

$$f_M = n_e\left(\frac{m_e}{2\pi k_B T_e}\right)^{\frac{3}{2}}\exp\left(-\frac{m_e|\mathbf{u}|^2}{2k_B T_e}\right). \tag{7}$$

In order to proceed, we define the *electron intensity operator* $\langle\rangle$ acting on a quantity g as

$$\langle g\rangle = \int_0^\infty g\,\frac{m_e}{2}|\mathbf{u}|^5\mathrm{d}|\mathbf{u}|. \tag{8}$$

This comes handy in definition of a new transported quantity

$$I^e = \int f^e |\mathbf{u}| \frac{m_e |\mathbf{u}|^2}{2} |\mathbf{u}|^2 \, \mathrm{d}|\mathbf{u}|, \tag{9}$$

which is referred to as the one-group electron intensity (the flux moment in the electron velocity magnitude $|\mathbf{u}|$ of the electron distribution function f^e).

Since we want to apply the transport model on the hydrodynamic time scale, we omit the time derivative of f^e in (6). Then, when the operator (8) is applied to Eq. (6), we can write the electron transport as

$$\mathbf{n} \cdot \nabla_{\mathbf{x}} \langle f^e \rangle - \frac{4q_e}{m_e} \mathbf{n} \cdot \mathbf{E} \left\langle \frac{f^e}{|\mathbf{u}|^2} \right\rangle = \frac{n_i}{n_e} \frac{\mathrm{d}\bar{Z}}{\mathrm{d}t} \left\langle \frac{f_M}{|\mathbf{u}|} \right\rangle + \left\langle \frac{f_M}{\lambda(|\mathbf{u}|^4)} \right\rangle - \left\langle \frac{f^e}{\lambda(|\mathbf{u}|^4)} \right\rangle, \tag{10}$$

where the second term on the left hand side results from the integration by parts and we have used $\lambda = \nu_e/|\mathbf{u}|$, which is a function of $|\mathbf{u}|^4$. The operator (8) applied to f_M reduces to the Gaussian integral, and so, we can obtain an explicit equality

$$\left\langle \frac{f_M}{\lambda(|\mathbf{u}|^4)} \right\rangle = \frac{\langle f_M \rangle}{8\lambda^e}, \tag{11}$$

which provides a definition of average values of the mean free path $8\lambda^e$ and the source $\langle f_M \rangle = \left(\frac{n_e}{\pi^{\frac{3}{2}}} \frac{\sqrt{2} k_B^{\frac{3}{2}}}{\sqrt{m_e}} \right) T_e^{\frac{3}{2}}$. An explicit evaluation of $\left\langle \frac{f_M}{|\mathbf{u}|} \right\rangle = \frac{3}{8\pi} n_e k_B T_e$ is also straightforward. Similarly, as in the construction (11), the other terms in (10) can be determined as

$$\left\langle \frac{f^e}{|\mathbf{u}|^2} \right\rangle \approx \frac{m_e \langle f^e \rangle}{4 k_B T_e}, \quad \left\langle \frac{f^e}{\lambda(|\mathbf{u}|^4)} \right\rangle \approx \frac{\langle f^e \rangle}{8\lambda^e}, \tag{12}$$

where f^e in the integrals on the left hand sides is approximated by f_M. Then, when used in (10) and along with (9), the nonlocal BGK electron transport model reads

$$\mathbf{n} \cdot \nabla I^e = n_i \frac{\mathrm{d}\bar{Z}}{\mathrm{d}t} \frac{3}{8\pi} k_B T_e + \frac{q_e}{k_B T_e} \mathbf{n} \cdot \mathbf{E} I^e + \frac{1}{8\lambda^e} \left[\left(\frac{n_e}{\pi^{\frac{3}{2}}} \frac{\sqrt{2} k_B^{\frac{3}{2}}}{\sqrt{m_e}} \right) T_e^{\frac{3}{2}} - I^e \right]. \tag{13}$$

All specific details of the nonlocal BGK electron transport model can be found in Sec. 2.3.3 of Ref. 72.

The *nonlocal electron transport closure* providing the energy flux reads

$$\mathbf{q}_e = \int_{4\pi} \mathbf{n} I^e \, \mathrm{d}\mathbf{n},$$

where I^e is the one group electron intensity computed from Eq. (13).

In conclusion, the main advantage of our model resides in solving directly the transport equation, in contrast to LMV[19] and AWBS[20] convolution models, which by definition relies on a small parameter approximation in the mean-free-path. The most relevant property of our model resides in the applicability to multi-dimensional geometries, while the convolution models (except from SNB[33]) by definition apply to 1D, which is also the case of the CMG model. Our model also addresses properly the question of anisotropy, since the momentum space of the transport direction is resolved by a high-order approximation. This makes our model to be superior to the moment method requiring a moment closure, where the level of anisotropy is limited by the model, e.g., P_1 (and its VEF variations).[47] Even though this has been further improved by the M_1 model[37,40] by maximizing the angular entropy, the moment closure does not arise from the original Boltzmann transport equation.

It should be stressed that the main advantage of our method resides in a cooperative symbiosis between the fundamental physics represented by a simplified form of the Boltzmann transport equation and the computational science represented by a high-order numerical scheme solving the linear transport equation in phase-space, see Appendix B. This provides a reasonable response to the nonlocal effect due to global temperature and density plasma profiles. It should also be noted that the use of the diffusive electric field Eq. (A5) in Eq. (13) is potentially dangerous. It is due to its strong effect on the heat flux (reduction of 50%–70%, see Appendix A), which can lead to a change of sign of the nonlocal (inhibited) heat flux if a *full* diffusive electric field is applied. Consequently, a further treatment of our nonlocal electron model proves to be useful. Based on the knowledge of the diffusion asymptotic of electron transport[9] (revised in Appendix A), we can adjust the mean free path in (13) in the way to match the diffusion limits of (A6) and (A8). Then, the *nonlocal BGK electron transport model* reads

$$\mathbf{n} \cdot \nabla I^e = \frac{\left(\frac{n_e}{\pi^{\frac{3}{2}}} \frac{\sqrt{2} k_B^{\frac{3}{2}}}{\sqrt{m_e}} \right) T_e^{\frac{3}{2}} - I^e}{\alpha \lambda_{SH}}, \tag{14}$$

where the original dependence on the plasma electric field $\mathbf{E}$ has been omitted; however, its effect is still included thanks to sharing the diffusion limit with the Spitzer-Harm heat flux (A6) and λ_{SH} is defined in (A7). This is reflected by the mean free path scaling parameter

$$\alpha(\bar{Z}) = \frac{64}{3\sqrt{2\pi}} \frac{\bar{Z} + 0.24}{\bar{Z} + 4.2}, \tag{15}$$

which provides an appropriate limit for low $\bar{Z}$ plasmas, where the electron-electron collisions become important.

We have also omitted the dependence of transport on the ionization rate in (14), since

$$\frac{n_i \frac{\mathrm{d}\bar{Z}}{\mathrm{d}t} \frac{3}{8\pi} k_B T_e}{\frac{\sqrt{2} m_e n_e}{\frac{64}{3\sqrt{2\pi}} \lambda_{SH} \pi^{\frac{3}{2}}} \left(\frac{k_B T_e}{m_e} \right)^{\frac{3}{2}}} \approx \frac{\frac{c_s}{L}}{\frac{\lambda_{SH}}{v_{th}}} \approx \mathrm{Kn}^e \frac{c_s}{v_{th}}, \tag{16}$$

where c_s is the hydrodynamic speed of sound ($\tau_h = L/c_s$ is the hydrodynamic time scale) and one can see that for high

temperature plasma and moderate nonlocality, the effect of ionization can be neglected.

IV. SIMULATIONS

An efficient and correct numerical implementation of the NTH model from Sec. III is the corner stone of the predictive laser plasma simulations and theoretical understanding of experiments. In principle, the original scheme of radiation transport Eq. (5) and its coupling to hydrodynamics were properly analyzed in Ref. 61. The essentials of this scheme for both radiation and electrons can be found in Sec. III B. Correspondingly, the nonlocal electron transport model Eq. (14) and its complex behavior can be benchmarked against the results of kinetic modeling. In what follows, the standard temperature decay Short-Epperlein[25] test and hotspot relaxation provide a better insight into the properties of the electron part of the NTH model. At the end of this section, an actual simulation of a laser heated plasma demonstrates the influence of the transport effect on the plasma ablation. All the simulations in this work were done using our developed Plasma Euler and Transport Equation hydrodynamic code (PETE).[61]

A. Short-Epperlein test

This test resides in a gradual decay of an initial periodic perturbation $\delta T \cos(kz)$ towards the base temperature $T_0 = 1000\,\mathrm{eV}$ due to the nonlocal electron transport flux of energy $\mathbf{q}_e$. Then, the asymptotic relaxation rate for $\delta T \ll T_0$ is observed ($\delta T = 10^{-4} \cdot T_0$), where the resulting energy fluxes expressed in terms of the effective heat conductivity $\kappa = |\mathbf{q}_e|/(kT_e)$ are calculated. Figure 1 shows the original Fokker-Planck (FP) results obtained by Short and Epperlein.[25,73] These kinetic simulations are further accompanied by classical nonlocal convolution transport models LMV[19] and AWBS[20] and by the results obtained with the PETE code actually solving Eq. (14) and referred to as PETE (NTH). The aim of this test is to show the dependency of the flux on the Knudsen number $k\lambda^e$, where λ^e is the thermal electron mean free path and k is the wave number, i.e., the inverse of the temperature scale length.

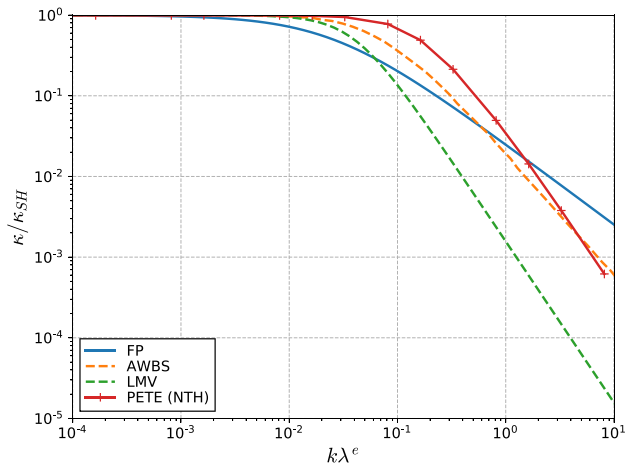

FIG. 1. Effective heat conductivities as a function of the Knudsen number $k\lambda^e$. Profiles for LMV, AWBS, and Fokker-Planck (FP) are taken from Ref. 25.

The test was conducted with constant $\lambda^e = 1.29 \times 10^{-6}\,\mathrm{cm}$ and varying k in the simulation area with 20 000 cells and the size $|z_{max} - z_{min}|$ adjusted to maintain the constant number of waves $|z_{max} - z_{min}|k = 2\pi \cdot 50$. At each point, the convergence in terms of the number of cells was verified and the time step was chosen sufficiently short to retain the evolution asymptotic, i.e., do not allow the temperatures to depart from the initial conditions significantly.

The results plotted in Fig. 1 show that the simulation code PETE provides a reasonable agreement with Fokker-Planck simulations. Similar to other nonlocal transport models for hydrodynamic simulations like LMV and AWBS,[22] our proposed model approaches the limit $(k\lambda^e)^{-2}$, and consequently, its validity for large Knudsen numbers is limited. It is worth noting that the AWBS model gives the results closest to the FP curve. The simplified kinetic equation that is the basis of this model arguably better describes the transport compared to the plain BGK operator and gives more complex dependencies of the propagators for the resulting convolution model.[20]

B. Hotspot relaxation problem

A more comprehensive test was published in Ref. 74, where the initially Gaussian profile of electron temperature with maximum 5 keV and base temperature 1 keV relaxes in time due to the effect of nonlocal electron transport. The sufficiently long time evolution allows us to analyze the transport in different transport regimes characterized by varying Knudsen numbers, where the transition from the nonlocal to diffusive regime can be observed. Figure 2 shows three different models: classical SH heat diffusion (orange line); 5% flux limited SH diffusion (blue line); and NTH model Eq. (14) (green line). The times and spatial coordinates are normalized to the electron–ion collision time τ_{ei} and the mean free path λ_{ei}, respectively, where $\tau_{ei} = 1.11\,\mathrm{ps}$ and $\lambda_{ei} = 15\,\mu\mathrm{m}$ at the base temperature.

At an early time $2\,\tau_{ei}$, the maximum Knudsen number is above one, i.e., leading to the nonlocal transport regime, where the classical SH diffusion model overestimates the actual heat flux. In particular, the flux limited diffusion and NTH model exhibit a strong flux inhibition (lower relaxation rate of temperature), which corresponds very well to the results of Vlasov–Fokker–Planck simulations with OSHUN[75] presented in Ref. 74. The same trend in the temperature profile can be seen at time $30\tau_{ei}$ (maximum Knudsen number approximately 0.1), where, however, the flux limited diffusion leads to an excessively strong transport inhibition.

The strong heat flux starvation in the case of flux-limited heat diffusion shows that flux limitation techniques may lead to nonphysical effects. However, our NTH model provides smooth temperature and flux profiles again in good agreement with the kinetic results presented in Ref. 74.

In general, we may conclude that the NTH model performs remarkably well, applying implicitly the heat flux inhibition in the early times for sharp temperature profiles and approaches the classical SH diffusion in the late times, while avoiding any nonphysical effects appearing due to the flux-limiting.

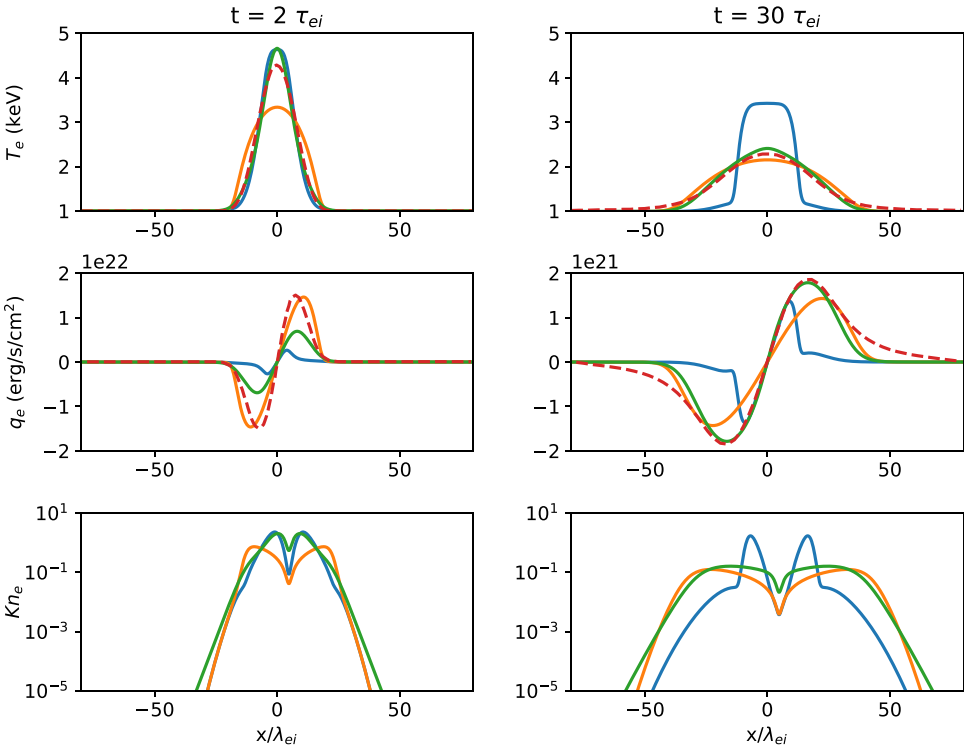

FIG. 2. Hotspot relaxation problem simulated with different models of energy transport. Profiles of electron temperatures T_e, electron heat fluxes q_e, and electron Knudsen numbers $Kn_e = \lambda^e|\nabla T_e|/T_e$ are shown. The blue line corresponds to the flux-limited heat diffusion with $f_{lim} = 0.05$, the orange line refers to the unlimited heat diffusion, and the green line to the nonlocal transport model. The results of kinetic simulations with OSHUN taken from Ref. 74 are plotted with the dashed red line.

C. Laser-target interaction

PETE currently implements the 1D formulation of our nonlocal transport hydrodynamic model presented in Sec. III, where the Euler equations are solved by using the staggered grid scheme[43] and the nonlocal transport equations for electrons and radiation are solved by our proposed high-order finite element DG-BGK&Ts scheme.[61] Each of the transported particles is treated as one energy group.

For the following simulations, we used a thick foil target (200 μm) made of CH plastic with $Z = 3.5$. The Lagrangian computational mesh consisted of 450 cells, where the first 3 μm were covered by 250 cells with a geometric factor of 0.975 (laser absorption takes place on a very fine mesh), and the remaining part of the target was spatially discretized by 200 cells with a geometric factor of 0.981.

The following configuration of the laser pulse is considered:

$$\lambda_L = 1.057\,\mu\text{m}, \quad I = 10^{14}\,\text{W/cm}^2, \quad \tau = 10\,\text{ns},$$

where λ_L is the Nd:glass laser pulse wave length and I the irradiating intensity, which is assumed to be constant along the laser pulse duration τ. An example of the laser-target interaction can be seen in Fig. 3. In principle, a several ns duration flat pulse irradiating a plastic target provides similar conditions to the direct drive inertial confinement fusion (ICF).

In order to address the dominant physical phenomena, we distinguish between four different regions[41] as they are naturally created during the laser plasma interaction as can be seen in Fig. 3 and in more detail in Fig. 4. The unaffected region of the target is labeled "0." At the beginning of the laser pulse, the energy is absorbed within a thin surface layer. This provides the material heating and a consequent increase in pressure, which leads to the hot plasma expansion (outward ablation). As a response to this expansion, a layer of a shocked material labeled "I" moving inward is then formed with a propagating shock wave on its face. The ablation front can be easily distinguished by the hydrodynamic flux $p\mathbf{v}$ orientation (wherever $p\mathbf{v} > 0$, plasma ablates), where p is the plasma pressure and $\mathbf{v}$ the plasma fluid velocity. As the hot material expands, the critical electron density n_{cr} is established at some point of the expanding plasma, and at a certain time, the critical density gets separated from the ablation front due to the transport properties of the plasma. Thus, a zone of a finite width is formed between the ablation front and where the laser energy is deposited. This finite region is labeled "II." The remaining part of the expanding plasma

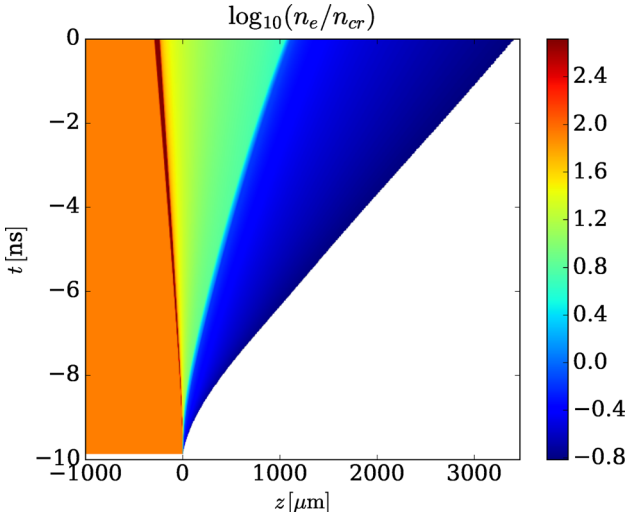

FIG. 3. The electron density profile formed during 10 ns of 10^{14} W/cm^2 intense laser pulse irradiating plastic target.

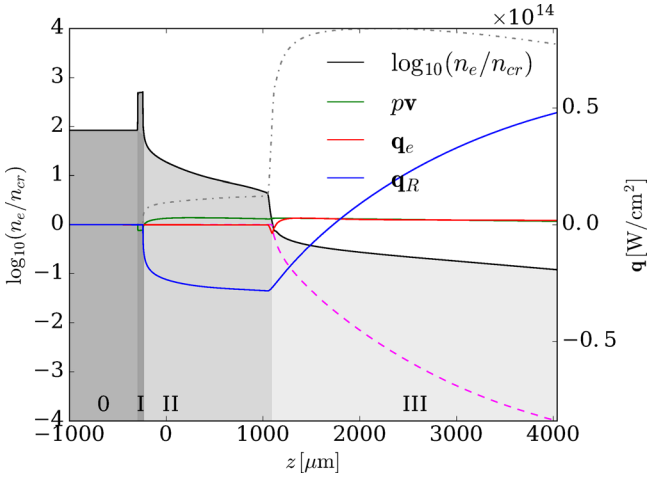

FIG. 4. The plasma profile after 10 ns of laser irradiation, where different zones are shown: 0 cold target; I shocked target; II conduction zone; and III plasma corona. The profiles of energy fluxes contributing to the energy equation (4) emphasize the dominance of each of the transport phenomena, i.e., fluid, electron, and radiation transport of energy, in each of the zones. Additionally, the dashed magenta line plots the profile of laser flux $\mathbf{q}_L$ and the dashed-dotted gray line the profile of electron temperature T_e with the minimum of 0.03 eV and the maximum of 985 eV.

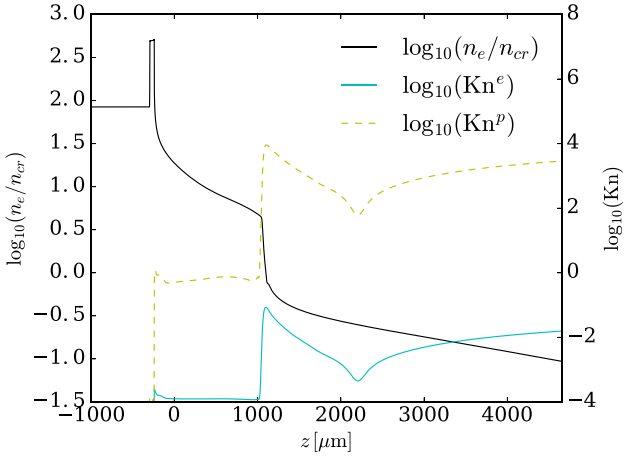

FIG. 5. Detailed profiles of electron and photon Knudsen numbers along the plasma profile on the log scale corresponding to the time 10 ns. It is worth mentioning that radiation transport is highly nonlocal even in the conduction zone, while electrons exhibit the strongest nonlocality in the proximity of critical density.

characterized by an under-critical electron density is labeled "III."

Since the main mechanism of energy transfer between the laser deposition region and the cold shell material is due to transport of energy (heat), region II is referred to as the conduction zone. The fluxes $\mathbf{q}_e$ and $\mathbf{q}_R$ play an important role in the fluid description by Euler's equations. As can be seen in Fig. 4, the hydrodynamic flux $p\mathbf{v}$ dominates in the compressed part of the target (zone "0"), and the radiation flux $\mathbf{q}_R$ is dominating in the conduction zone "II," while the laser flux $\mathbf{q}_L$ prevails in the zone "III." It is worth mentioning that the effectiveness of the transport is best described by the flux divergence, and consequently, the nonlocal electron transport contributes to the energy equation (4) mostly around the critical density, i.e., at the interface between zones "II" and "III." The entire picture of the nonlocal energy transport effect is presented in Fig. 5, where the actual Knudsen number of electrons and photons is plotted with respect to the electron density profile of the expanding plasma.

In order to conclude, it is clear that both electrons and radiation nonlocal description play an important role in the ablative physics, since the electron Knudsen numbers range between $0.001 < \mathrm{Kn}^e < 0.1$ in the plasma corona and the highest values correspond to the critical density region, and the photon Knudsen number ranges $1 < \mathrm{Kn}^p < 10^4$ everywhere the plasma ablates, i.e., radiation transport is significantly nonlocal even in the conduction zone.

V. CONCLUSIONS

The nonlocal transport hydrodynamic model proposed in this work provides a general tool for simulations of laser heated plasmas. On the basis of advanced numerical methods, it can describe properly the sensitive physics related to transport properties of plasma on microscopic scales, where a classical fluid description is not sufficient, yet simple enough to be efficiently computed during long ns laser pulse experiments. Its validity under varying Knudsen numbers has been demonstrated on two test cases, and the actual effect of nonlocal transport appears naturally in the simulation of the laser-target interaction similar to direct-drive ICF conditions. We are well aware of the diversity of transport physics with respect to the energy spectra of either electrons and photons, and consequently, we plan to extend our model to include the multi-group approach. This will be, however, the next step in the model development in the future. Moreover, the simplicity of the form of the BGK collision operator enables us to extend the model beyond the classical collision theory and describe the qualitative behaviour of the matter in highly non-ideal plasma states, provided that the operator can be still considered a linearization of the transport mechanisms with appropriate relaxation rates. On the other hand, the properties of the model in a classical plasma can be improved by a more accurate linear collision operator like AWBS as it was observed in Sec. IV A. In both cases, we set out extension of the model and construction of an appropriate closure model as prospects of our future work.

ACKNOWLEDGMENTS

This work was supported by project ELITAS (CZ.02.1.01/0.0/0.0/16 013/0001793) and project HiFI (CZ.02.1.01/0.0/0.0/15 003/0000449) both from European Regional Development Fund, Czech Technical University Grant No. SGS16/247/OHK4/3T/14 and EUROfusion Project No. CfP-AWP17-IFE-CEA-01.

APPENDIX A: DIFFUSIVE ELECTRON TRANSPORT

It can be observed that electron-ion collisions simplify significantly if defined in spherical coordinates of velocity and the assumption $m_e/m_1 \ll 1$ is applied, because the dominant electron-ion Landau-Fokker-Planck operator then reduces to

$$C_{ei}(f^e) \overset{m_e/m_i}{\approx} \sigma n_i \nabla_{\mathbf{v}} \cdot \left[\frac{1}{|\mathbf{u}|} \left(\mathbf{I} - \frac{\mathbf{v} \otimes \mathbf{v}}{|\mathbf{u}|^2} \right) \cdot \nabla_{\mathbf{v}} f^e \right] \overset{\text{spher}}{\approx} \frac{\sigma n_i}{|\mathbf{u}|^3} \frac{1}{\sin(\phi)} \left[\frac{\partial}{\partial \phi} \left(\sin(\phi) \frac{\partial f^e}{\partial \phi} \right) + \frac{1}{\sin(\phi)} \frac{\partial^2 f^e}{\partial \theta^2} \right], \tag{A1}$$

where f^e is the electron distribution function and $\sigma = 4\pi \bar{Z}^2 e^4 \ln\Lambda / m_e$. Now, the action of (A1) on the lowest anisotropy approximation of the electron distribution function

$$\tilde{f}^e = f_0^e + f_1^e \cos(\phi) \tag{A2}$$

leads to the definition of a low anisotropy Landau-Fokker-Planck collision operator approximation

$$C_{ei}(\tilde{f}^e) \approx \frac{1}{\sin(\phi)} \frac{\partial}{\partial \phi} \left[\sin(\phi) \frac{\partial \tilde{f}^e}{\partial \phi} \right] = -\frac{2\sigma n_i}{|\mathbf{u}|^3} f_1^e \cos(\phi) = \frac{2\sigma n_i}{|\mathbf{u}|^3} \left(f_0^e - \tilde{f}^e \right), \tag{A3}$$

which provides a direct interpretation of the well known BGK operator making an assumption that $f_0 \approx f_M$, i.e., $C_{BGK}(f) = (f_M - f)/\lambda$, where $\lambda = |\mathbf{u}|^4 / 2\sigma n_i$.

The low anisotropy approximation (A2) can be then expressed from the Boltzmann transport equation equipped with simplified electron-ion collisional operator (A1) [under low anisotropy equivalent to the BGK operator (A3)] as

$$f_{SH}(\mathbf{x}, |\mathbf{u}|, \mathbf{n}) = f_M - \lambda \xi^0 \mathbf{n} \cdot \left[\left(\frac{|\mathbf{u}|^2}{2 v_{th}^2} - 4 \right) \frac{\nabla T_e}{T_e} f_M \right], \tag{A4}$$

where $\xi^0(\bar{Z}) = \frac{\bar{Z}+0.24}{\bar{Z}+4.2}$ is a correction to mean free path due to the electron-electron collisions.[9] The zero current condition and its dependence on $\bar{Z}$ correspond to Spitzer electric field

$$\mathbf{E}_{SH} = \frac{k_B T_e}{q_e} \left(\frac{\nabla n_e}{n_e} + \xi^1 \frac{\nabla T_e}{T_e} \right), \tag{A5}$$

where $\xi^1(\bar{Z}) = 1 + \frac{3}{2} \frac{\bar{Z}+0.477}{\bar{Z}+2.15}$.[9] The Spitzer-Harm heat flux then takes the form

$$\mathbf{q}_{SH} = \int_{4\pi} \int_0^\infty \frac{m_e |\mathbf{u}|^2}{2} |\mathbf{u}| \mathbf{n} f_{SH} |\mathbf{u}|^2 \, \mathrm{d}|\mathbf{u}| \, \mathrm{d}\mathbf{n} = \frac{128}{\sqrt{2\pi}} \xi^0 \frac{v_{th}^4}{\sigma n_i} v_{th} n_e k_B \nabla T_e = \frac{128}{3\pi} \frac{\bar{Z} + 0.24}{\bar{Z} + 4.2} \lambda_{SH} v_{th} n_e k_B \nabla T_e, \tag{A6}$$

where the *Spitzer-Harm mean free path* reads[9]

$$\lambda_{SH} = \frac{3 v_{th}^4 m_e}{4\sqrt{2\pi} \bar{Z} e^4 n_e \ln\Lambda}. \tag{A7}$$

In (A6), the values $1.7 \leq \xi^1 \leq 2.5$ provide that the electric field reduces the *neutral* heat flux ($\xi^1 = 0$) of ≈50% in the case of low $\bar{Z} = 1$ and of ≈70% in the case of high $\bar{Z} \to \infty$ plasmas.

A similar diffusion asymptotic can be obtained in the case of our nonlocal BGK electron transport (14), while applying $I^e_{diff} \approx I_0 + I_1 \cos(\phi)$. Consequently, the intensity behaves as

$$I^e_{diff}(\mathbf{x}, \mathbf{n}) = I_M - \alpha \lambda_{SH} \mathbf{n} \cdot \nabla I_M,$$

where $I_M = \frac{n_e}{\pi^{3/2}} \frac{\sqrt{2} k_B^{3/2}}{\sqrt{m_e}} T_e^{3/2}$ and the corresponding heat flux in the diffusive regime of our electron transport model (14) can be expressed as

$$\mathbf{q}_e^{diff} = \int_{4\pi} \mathbf{n} I^e_{diff} \, \mathrm{d}\mathbf{n} = \alpha \frac{2^{3/2}}{\sqrt{\pi}} \lambda_{SH} v_{th} n_e k_B \nabla T_e, \tag{A8}$$

where $\nabla n_e = \mathbf{0}$ for simplicity. Then, it is straightforward to find the mean free path scaling parameter α [its explicit form (15)] while comparing (A6) to (A8)).

APPENDIX B: NONLOCAL TRANSPORT CLOSURE IMPLEMENTATION

The corner stone of the implementation of our nonlocal model resides in a discrete solution of the electron transport equation (14) and of the radiation transport equation (5), where the discrete analog can be written as

$$\mathbf{D} \cdot \mathbf{I} = \mathbf{S} \cdot \mathbf{T} - k \mathbf{M} \cdot \mathbf{I}, \tag{B1}$$

where $\mathbf{I}$ and $\mathbf{T}$ are discrete finite element representation of their continuous counterparts $I(\mathbf{x}, \mathbf{n})$ and $T_e(\mathbf{x})$, and matrices $\mathbf{D}$, $\mathbf{S}$, and $\mathbf{M}$ are discrete finite element bilinear forms representing the continuous transport and BGK collision operators. After some algebraic operations, the discrete solution of (B1) can be found in the form

$$\mathbf{I} = \mathbf{A} \cdot \mathbf{T} + \mathbf{b}, \tag{B2}$$

i.e., a discretized linear function of electron temperature.[61] The matrix coefficient $\mathbf{A}(t, \mathbf{x}, \mathbf{n})$ and vector $\mathbf{b}(t, \mathbf{x}, \mathbf{n})$ depend on time t, mesh coordinates $\mathbf{x}$, and transport direction $\mathbf{n}$. Taking into account that $\mathbf{b}$ includes inter-element exchange terms essential for non-locality of the model, we are actually solving the phase-space kinetic problem, except for the dimension corresponding to energy of the transported species.

Finally, the nonlocal transport closure reads

$$\mathbf{q}_e + \mathbf{q}_R = \int_{4\pi} \mathbf{n} \left(\mathbf{I}^e + \mathbf{I}^p \right) \mathrm{d}\mathbf{n} = \mathbf{A}_\mathbf{q} \cdot \mathbf{T} + \mathbf{b}_\mathbf{q}, \tag{B3}$$

where the sum of electron heat flux and radiation energy flux $\mathbf{q}_e + \mathbf{q}_R$ is written as a function of discrete electron temperature $\mathbf{T}$ under the operation of matrices $\mathbf{A}_\mathbf{q}(\mathbf{x})$ and $\mathbf{b}_\mathbf{q}(\mathbf{x})$ as a result of directional integration of the electron discrete solution $\mathbf{I}^e$ of Eq. (14) and the radiation discrete solution $\mathbf{I}^p$ of Eq. (5), both expressed in the form (B2).

More details about the discrete solution (B3), its accuracy for arbitrary mean free path and appropriate convergence to the heat conduction when coupled to temperature equation (when $\lambda^{e,p} \to 0$) can be found in Ref. 61.

[1]D. Mihalas and B. Mihalas, *Foundations of Radiation Hydrodynamics* (Oxford University Press, New York, 1985).
[2]J. Castor, *Radiation Hydrodynamics* (Cambridge University Press, Cambridge, 2004).
[3]Y. Zeldovich and Y. Raizer, *Physics of Shock Waves and High-Temperature Hydrodynamic Phenomena* (Dover Publications, New York, 2002).
[4]S. Atzeni and J. Meyer-Ter-Vehn, *The Physics of Inertial Fusion* (Clarendon Press, Oxford, 2004).
[5]P. Bhatnagar, E. Gross, and M. Krook, Phys. Rev. **94**, 511 (1954).
[6]A. V. Brantov and V. Y. Bychenkov, Plasma Phys. Rep. **39**, 698 (2013).
[7]S. Chapman and T. G. Cowling, *Mathematical Theory of Nonuniform Gases* (Cambridge University Press, Cambridge, 1952).
[8]R. S. Cohen, L. Spitzer, Jr., and P. M. Routly, Phys. Rev. **80**, 230 (1950).
[9]J. L. Spitzer and R. Harm, Phys. Rev. **89**, 977 (1953).
[10]R. C. Malone, R. L. McCrory, and R. L. Morse, Phys. Rev. Lett. **34**, 721 (1975).
[11]M. D. Rosen, D. W. Phillion, V. C. Rupert, W. C. Mead, W. L. Kruer, J. J. Thomson, H. N. K. V. W. Slivinsky, G. J. Caporaso, M. J. Boyle, and K. Tirsell, Phys. Fluids **22**, 2020 (1979).
[12]A. Sunahara, J. A. Delettrez, C. Stoeckl, R. W. Short, and S. Skupsky, Phys. Rev. Lett. **91**, 095003 (2003).
[13]D. G. Colombant, W. M. Manheimer, and M. Busquet, Phys. Plasmas **12**, 072702 (2005).
[14]A. R. Bell, R. G. Evans, and D. J. Nicholas, Phys. Rev. Lett. **46**, 243 (1981).
[15]J. P. Matte and J. Virmont, Phys. Rev. Lett. **49**, 1936 (1982).
[16]E. M. Epperlein and R. Short, Phys. Fluids B **4**, 2211 (1992).
[17]V. Senecha, A. Brantov, V. Bychenkov, and V. Tikhonchuk, Phys. Rev. E **57**, 978 (1998).
[18]O. Batishchev, V. Bychenkov, F. Detering, W. Rozmus, R. Sydora, C. Capjack, and V. Novikov, Phys. Plasmas **9**, 2302 (2002).
[19]J. F. Luciani, P. Mora, and J. Virmont, Phys. Rev. Lett. **51**, 1664 (1983).
[20]J. R. Albritton, E. A. Williams, I. B. Bernstein, and K. P. Swartz, Phys. Rev. Lett. **57**, 1887 (1986).
[21]A. Bendib, J. F. Luciani, and J. P. Matte, Phys. Fluids **31**, 711 (1988).
[22]M. K. Prasad and D. S. Kershaw, Phys. Fluids B **1**, 2430 (1989).
[23]M. K. Prasad and D. S. Kershaw, Phys. Fluids B **3**, 3087 (1991).
[24]E. M. Epperlein, Phys. Rev. Lett. **65**, 2145 (1990).
[25]E. M. Epperlein and R. W. Short, Phys. Fluids B **3**, 3092 (1991).
[26]V. T. V. Yu. Bychenkov and W. Rozmus, Phys. Rev. Lett. **75**, 4405 (1995).
[27]A. Brantov, V. Bychenkov, V. Tikhonchuk, and W. Rozmus, J. Exp. Theor. Phys. **83**, 716 (1996).
[28]A. Brantov, V. Bychenkov, V. Tikhonchuk, and W. Rozmus, Phys. Plasmas **5**, 2742 (1998).
[29]V. Bychenkov, V. N. Novikov, and V. Tikhonchuk, J. Exp. Theor. Phys. **87**, 916 (1998).
[30]S. Weber, G. Riazuelo, P. Michel, R. Loubere, F. Walraet, V. T. Tikhonchuk, V. M. J. Ovadia, and G. Bonnaud, Laser Part. Beams **22**, 189 (2004).
[31]S. Weber, P. Maire, R. Loubere, G. Riazuelo, P. Michel, V. Tikhonchuk, and J. Ovadia, Comput. Phys. Commun. **168**, 141 (2005).
[32]D. del Castillo-Negrete, Phys. Plasmas **13**, 082308 (2006).
[33]G. Schurtz, P. Nicolai, and M. Busquet, Phys. Plasmas **7**, 4238 (2000).
[34]P. D. Nicolai, J.-L. A. Feugeas, and G. P. Schurtz, Phys. Plasmas **13**, 032701 (2006).
[35]G. Schurtz, S. Gary, S. Hulin, C. Chenais-Popovics, J.-C. Gauthier, F. Thais, J. Breil, F. Durut, J.-L. Feugeas, P.-H. Maire, P. Nicola, O. Peyrusse, C. Reverdin, G. Soulli, V. Tikhonchuk, B. Villette, and C. Fourment, Phys. Rev. Lett. **98**, 095002 (2007).
[36]D. D. Sorbo, J.-L. Feugeas, P. Nicolai, M. Olazabal-Loume, B. Dubroca, S. Guisset, M. Touati, and V. Tikhonchuk, Phys. Plasmas **22**, 082706 (2015).
[37]B. Dubroca, J.-L. Feugeas, and M. Frank, Eur. Phys. J. D **60**, 301 (2010).
[38]M. Touati, J.-L. Feugeas, P. Nicolai, J. Santos, L. Gremillet, and V. Tikhonchuk, New J. Phys. **16**, 073014 (2014).
[39]D. D. Sorbo, J.-L. Feugeas, P. Nicolai, M. Olazabal-Loume, B. Dubroca, and V. Tikhonchuk, Laser Part. Beams **34**, 412 (2016).
[40]G. N. Minerbo, J. Quant. Spectrosc. Radiat. Transfer **20**, 541 (1978).
[41]V. N. Goncharov, O. V. Gotchev, E. Vianello, T. R. Boehly, J. P. Knauer, P. W. McKenty, P. B. Radha, S. P. Regan, T. C. Sangster, S. Skupsky, V. A. Smalyuk, R. Betti, R. L. McCrory, D. D. Meyerhofer, and C. Cherfils-Clrouin, Phys. Plasmas **13**, 012702 (2006).
[42]W. Manheimer, D. Colombant, and V. Goncharov, Phys. Plasmas **15**, 083103 (2008).
[43]M. Shashkov, *Conservative Finite-Difference Methods on General Grids* (CRC Press, Boca Raton, 1996).
[44]S. Rosseland, *Theoretical Astrophysics* (Oxford University Press, Oxford, 1936).
[45]K. H. Simmons and D. Mihalas, J. Quant. Spectrosc. Radiat. Transfer **66**, 263 (2000).
[46]G. L. Olson, L. H. Auer, and M. L. Hall, "Diffusion, P1, and other approximate forms of radiation transport," Technical Report No. LA-UR-99-471 (Los Alamos National Laboratory, Los Alamos, NM, 2000).
[47]B. E. Freeman, L. E. Hauser, J. T. Palmer, S. Pickard, G. M. Simmons, D. G. Williston, and J. E. Zerkle, "The VERA code: A one dimensional radiation hydrodynamics code," Technical Report No. 2135 (DASA, La Jolla: Systems, Science, and Software, Inc., 1968), Vol. I.
[48]D. S. Kershaw, "Flux limiting nature's own way," Technical Report No. UCRL-78378 (Lawrence Livermore National Laboratory, 1976).
[49]B. G. Carlson, "Solution of the transport equation by Sn approximations," Technical Report No. LA-1599 (Los Alamos National Laboratory, Los Alamos, NM, 1953).
[50]G. C. Pomraning, *The Equations of Radiation Hydrodynamics* (Pergamon Press, Oxford, 1973).
[51]P. G. Dykema, R. I. Klein, and J. I. Castor, Astrophys. J. **457**, 892 (1996).
[52]M. Adams, Transp. Theory Stat. **26**, 385 (1997).
[53]M. Adams, Nucl. Sci. Eng. **137**, 298 (2001).
[54]M. Adams and E. Larsen, Prog. Nucl. Energy **40**, 3 (2002).
[55]L. Mieussens, J. Comput. Phys. **162**, 429 (2000).
[56]Y. Wang and J. C. Ragusa, Ann. Nucl. Energy **36**, 931 (2009).
[57]R. Sanchez and J. Ragusa, Nucl. Sci. Eng. **169**, 133 (2011).
[58]A. Alekseenko, Appl. Numer. Math. **61**, 410 (2011).
[59]A. Alekseenko, N. Gimelshein, and S. Gimelshein, Int. J. Comput. Fluid Dyn. **26**, 145 (2012).
[60]Y. Cheng, I. Gamba, F. Li, and P. Morrison, SIAM J. Numer. Anal. **52**, 1017 (2014).
[61]M. Holec, J. Limpouch, R. Liska, and S. Weber, Int. J. Numer. Methods Fluids **83**, 779 (2017).
[62]T. Group, "SESAME report on the Los Alamos equation-of-state library," Technical Report No. LALP-83-4 (Los Alamos National Laboratory, Los Alamos, 1983).
[63]S. P. Lyon and J. D. Johnson, "SESAME: The Los Alamos National Laboratory equation of state database," Technical Report No. LA-UR-92-3407 (Los Alamos National Laboratory, Los Alamos, 1992).
[64]Y. V. Afanas, N. N. Demchenko, O. N. Krokhin, and V. B. Rosanov, Zh. Eksp. Teor. Fiz. **72**, 170 (1977).
[65]M. Born and E. Wolf, *Principles of Optics: Electromagnetic Theory of Propagation, Interference and Diffraction of Light* (Cambridge University Press, 1999), pp. 1–952.
[66]K. Eidmann, J. Meyer-ter Vehn, T. Schlegel, and S. Hüller, Phys. Rev. E **62**, 1202 (2000).
[67]Y. T. Lee and R. M. More, Phys. Fluids **27**, 1273 (1984).
[68]N. W. Ashcroft and N. D. Mermin, *Solid State Physics* (Saunders College, Philadelphia, 1976).
[69]H. M. Milchberg, R. R. Freeman, and S. C. Davey, Phys. Rev. Lett. **61**, 2364 (1988).
[70]J. Rubiano, R. Rodriguez, J. Gil, R. Florido, P. Martel, M. Mendoza, D. Suarez, and E. Minguez, J. Phys.: Conf. Ser. **112**, 042006 (2008).
[71]T. Heltemes and G. Moses, Comput. Phys. Commun. **183**, 2629 (2012).
[72]M. Holec, "Numerical modeling of nonlocal energy transport in laser-heated plasmas," Ph.D. thesis, Czech Technical University, Prague, 2016.
[73]E. M. Epperlein, Phys. Plasmas **1**, 109 (1994).
[74]A. Marocchino, M. Tzoufras, S. Atzeni, A. Schiavi, P. Nicolai, J. Mallet, V. Tikhonchuk, and J.-L. Feugeas, Phys. Plasmas **20**, 022702 (2013).
[75]M. Tzoufras, A. R. Bell, P. A. Norreys, and F. S. Tsung, J. Comput. Phys. **230**, 6475 (2011).